

# Contents

3.	The scattering approach	1
3.1	Introduction: From macroscopic wires to atomic-scale junctions . . . . .	1
3.2	Conductance is transmission: Heuristic derivation of the Landauer formula . . . . .	5
3.3	Penetration of a potential barrier: Tunnel effect . . . . .	8
3.4	The scattering matrix . . . . .	12
3.4.1	Definition and properties of the scattering matrix	13
3.4.2	Combining scattering matrices . . . . .	16
3.5	Resonant tunneling . . . . .	17
3.6	Multichannel Landauer formula . . . . .	18
3.6.1	Conductance quantization in 2DEG: Landauer formula at work . . . . .	23
3.7	Final remarks and limitations of the scattering approach .	25
3.8	Exercises . . . . .	26
	<i>Bibliography</i>	31

## Chapter 3

# The scattering approach to phase-coherent transport in nanocontacts

In this chapter we shall introduce the scattering (or Landauer) approach, which is presently the most popular theoretical formalism to describe the coherent transport in nanodevices. The central idea of this approach, already put forward by Rolf Landauer in the late 1950's [1], is that if one can ignore inelastic interactions, a transport problem can always be viewed as a scattering problem. This means in practice that transport properties like the electrical conductance are intimately related to the transmission probability for an electron to cross the system, which is often a quantity that can be easily computed with standard quantum-mechanical methods. Our introduction here to the scattering approach will be divided into two main parts. First, using heuristic arguments we shall show the relation between conductance and transmission, which is summarized in the so-called Landauer formula. This formula will then be used to discuss basic concepts such as a resonant transport. Second, we shall present a more rigorous formulation of this approach that will be used to compute the electrical conductance. Finally, we shall conclude this chapter with a discussion of the limitations of the scattering formalism. On the other hand, Appendix B presents an extension of the scattering formalism to analyze other transport properties such as the so-called shot noise or the thermoelectric coefficients.

### 3.1 Introduction: From macroscopic wires to atomic-scale junctions

The electrical conduction in macroscopic metallic wires is described by Ohm's law, which establishes that the current is proportional to the applied voltage. The constant of proportionality is simply the conductance,  $G$ , which for a given sample grows linearly with the transverse area  $S$  and

it is inversely proportional to its length  $L$ , i.e.

$$G = \sigma \frac{S}{L}, \quad (3.1)$$

where  $\sigma$  is the conductivity of the sample, which is a material specific property.<sup>1</sup> In a macroscopic wire the conductivity is mainly determined by two mechanisms: (i) the scattering of electrons with impurities (or defects, dislocations, etc.), which gives a contribution to the conductance that is temperature-independent, and (ii) the electron-phonon interaction, which is responsible for the  $1/T$  dependence of the conductance at room temperature, where  $T$  is the temperature.

The conductance will be a key quantity in our analysis of the transport properties of atomic and molecular junctions. However, concepts like Ohm's law are no longer applicable at the atomic scale and the mechanisms dominating the transport will also have little to do with those mentioned in the previous paragraph. Atomic-scale conductors are a limiting case of mesoscopic systems in which quantum coherence plays a central role in the transport properties. In mesoscopic systems one can identify different transport regimes according to the relative size of various length scales. These scales are, in turn, determined by different scattering mechanisms. A fundamental length scale is the *phase-coherence length*,  $L_\varphi$ , which measures the distance over which the information about the phase of the electron wave function is preserved. Phase coherence can be destroyed by inelastic scattering mechanisms such as electron-electron and electron-phonon interactions. Scattering of electrons by magnetic impurities, with internal degrees of freedom, also degrades the phase but elastic scattering by (static) non-magnetic impurities does not affect the coherence length. Information on the coherence length can be obtained experimentally, for instance, by studying the so-called weak localization [2]. A typical value for Au at  $T = 1$  K is around  $1 \mu\text{m}$ , while at room temperature it becomes of the order of a few tens of nm. The mesoscopic regime is determined by the condition  $L < L_\varphi$ , where  $L$  is a typical length scale of our sample.

Another important length scale is the elastic mean free path  $\ell$ , which roughly measures the distance between elastic collisions with static impurities. The regime  $\ell \ll L$  is called *diffusive*. In a semi-classical picture the electron motion in this regime can be viewed as a random walk of step

<sup>1</sup>You are probably more used to discussing the electric conduction in metallic wires in terms of the resistance  $R$ , which is simply the inverse of the conductance ( $R = 1/G$ ). You will learn later in this chapter why in the context of nanocontacts it is more convenient to use the conductance.

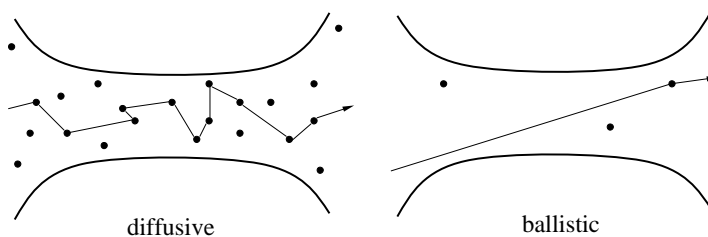


Fig. 3.1 Schematic illustration of a diffusive (left) and ballistic (right) conductor.

size  $\ell$  among the impurities. On the other hand, when  $\ell > L$  we reach the *ballistic* regime in which the electron momentum can be assumed to be constant and only limited by scattering with the boundaries of the sample. These two regimes are illustrated in Fig. 3.1.

In the previous discussion we have implicitly assumed that the typical dimensions of the sample are much larger than the Fermi wavelength  $\lambda_F$ , which in a metal is of the order of the interatomic distance. However, when dealing with atomic-scale junctions the contact width  $W$  is of the order of a few nanometers or even less and thus we have  $W \sim \lambda_F$ . We thus enter into the *full quantum* limit which cannot be described by semi-classical arguments. A main challenge for the theory is to derive the conductance of an atomic-scale conductor from microscopic principles. This is indeed what the theory part of this course is all about.

Let us now briefly revise the history to see how the transport in metallic contacts of reduced dimensions has been described in the past. On the basis of Ohm's law one would expect the conductance of a metallic wire to scale as  $R^2$ , where  $R$  is its radius. Deviations from such a scaling law were already discussed by Maxwell [3], who studied with classical arguments the conductance of a diffusive constriction, where the contact radius is large compared to the mean free path. He found that the conductance scales linearly with the contact radius, i.e.

$$G = 2R\sigma. \quad (3.2)$$

where  $\sigma$  is the conductivity.

As we shrink a conductor to well below the mean free path, the conductance departs from the value expected from the previous expression. In 1965 Sharvin [4] considered the propagation of electrical current through a ballistic contact by approximating it with a classical problem of dilute gas flow through an orifice. He reasoned that if the potential difference be-

tween the two half-spaces is  $eV$ , the conduction electrons passing through the orifice should change their velocity by the amount  $\Delta v = \pm eV/p_F$ , where  $p_F$  is the Fermi momentum.<sup>2</sup> The net current will be  $I = ne\Delta vS$ , where  $S = \pi R^2$  is the contact area and taking into account the Fermi-Dirac statistics for electrons,  $n = 4\pi p_F^3/(3h^3)$ , one gets the conductance for a circular ballistic point-contact

$$G = \frac{2e^2}{h} \left( \frac{\pi R}{\lambda_F} \right)^2 = \frac{2e^2}{h} \left( \frac{k_F R}{2} \right)^2, \quad (3.3)$$

where  $e$  is the electron charge and  $h$  is the Planck's constant. Notice that for ballistic contacts the conductance is proportional to the contact area, like in Ohm's law, but the proportionality constant  $2e^2/h$  has a quantum nature. An important difference between the two lies in the fact that  $G$  is independent of the length of the conductor and is determined only by its cross-section radius  $R$ . It is remarkable that the Sharvin formula, being based on semiclassical arguments, holds well for all ballistic contacts with diameters down to a few nanometers. In the context of atomic contacts, it is customary to use a slightly modified version of this equation in which the so-called Weyl correction is introduced [5]. This correction comes from the fact that the Heisenberg uncertainty principle for Fermi electrons in a narrow contact,  $2p_F R \geq \hbar$ , gives a small correction to the conductance and the resulting semiclassical formula takes the form

$$G = \frac{2e^2}{h} \left( \frac{k_F R}{2} \right)^2 \left( 1 - \frac{2}{k_F R} + \dots \right), \quad (3.4)$$

where  $k_F$  is the wave vector. This equation is valid for a contact in the form of a wire. For an orifice the numerator of the last fraction should be 1 instead of 2. Eq. (3.4), valid for contacts down to a few nanometers in diameter [6], is often used to establish the relationship between the conductance and the radius of a contact.

Due to limitations of the semiclassical approach, Eq. (3.4) does not account for purely quantum effects which dominate when the size of the contact becomes so small that the wave nature of an electron can no longer be ignored. Rolf Landauer [1] showed, already back in the 1950's, that in the latter case "conductance is transmission", i.e. in order to determine the total conductance one has to solve the Schrödinger equation, find the current-carrying eigenmodes, calculate their transmission values and sum

<sup>2</sup>This is just an approximation and the exact treatment includes an integration of the projection of  $\Delta v$  along the orifice axis over the solid angle of  $2\pi$ . Anyway, the phenomenological result is only a factor 8/3 different from the exact one.

up their contributions. Mathematically, this is summarized by in the Landauer formula

$$G = \frac{2e^2}{h} \sum_{n=1}^N T_n, \quad (3.5)$$

where the summation is performed over all available conduction modes and  $T_n$  are their individual transmissions. If the transmission of a mode is perfect, it contributes exactly one quantum unit of conductance,  $G_0 = 2e^2/h \sim (12.9 \text{ k}\Omega)^{-1}$ . This formula shows that by changing the size of the contact, one can change the number of modes contributing to the conductance and thus the conductance itself in a step-like manner (see discussion below). This is clearly at variance with the situations described above. Don't worry if you do not understand this formula now, its derivation and the discussion of its physical implications is the main subject of the rest of this chapter.

### 3.2 Conductance is transmission: Heuristic derivation of the Landauer formula

In a typical transport experiment on a nanoscale device, the sample is connected to macroscopic electrodes by a set of *leads* (or electrodes) which allow us to inject currents and fix voltages. The electrodes act as ideal electron reservoirs in thermal equilibrium with a well-defined temperature and chemical potential. The basic idea of the scattering approach is to relate the transport properties with the transmission and reflection probabilities for carriers incident on the sample. In this one-electron approach phase-coherence is assumed to be preserved on the entire sample and inelastic scattering is restricted to the electron reservoirs only. Instead of dealing with complex processes taking place inside the reservoirs, they enter into the description as a set of boundary conditions. In spite of its simplicity, this approach has been very successful in explaining many experiments on nanodevices.

Before turning to the description of the general scattering formalism, it is instructive to understand the relation between current and transmission with a simple heuristic argument. Let us consider a one-dimensional situation, like the one depicted in Fig. 3.2. Here, the potential simulates the central part of a junction, where electrons are elastically scattered before reaching one of the electrodes. We assume that when the electrons are inside the reservoirs, they are in thermal equilibrium at the temperature of

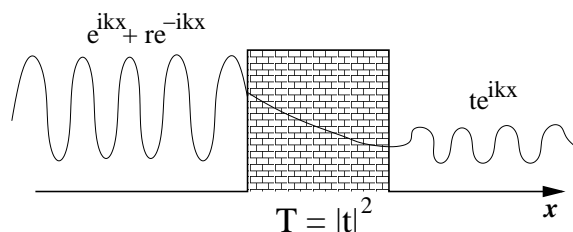


Fig. 3.2 Wave function (plane wave) impinging on a potential barrier. The wave is partially reflected with a probability amplitude  $r$  and partially transmitted with a probability  $T = |t|^2$ .

the corresponding electrode. Let us now consider a plane wave,  $(1/\sqrt{L})e^{ikx}$ , that is impinging on the potential barrier from the left ( $L$  represents the length of the system). This wave is partially reflected with a probability amplitude  $r$  and partially transmitted with a probability  $T = |t|^2$ . We can now compute the electrical current density,  $J_k$ , carried by an electron described by this wave function. It is given by the quantum-mechanical expression

$$J_k = \frac{\hbar}{2mi} \left[ \psi^*(x) \frac{d\psi}{dx} - \psi(x) \frac{d\psi^*}{dx} \right] = \frac{e}{L} v(k) T(k), \quad (3.6)$$

where  $v(k) = \hbar k/m$  is the group velocity and we have computed the current on the right hand side of the scattering potential (remember that the current is conserved and thus its value is independent of where it is evaluated).

In a solid state device there are many electrons contributing to the current. Therefore, we have to introduce a sum over  $k$  (strictly speaking over the positive values). Moreover, we have to take into account the Pauli principle, which means in practice that we have to introduce a factor  $f_L(k)[1 - f_R(k)]$ , where  $f_{L,R}$  is the Fermi function of the electron reservoir on the left ( $L$ ) or on the right ( $R$ ) of the potential barrier. These Fermi functions take also into account the fact that the corresponding chemical potential can be shifted by an applied bias voltage,  $V$ . The blocking factor above ensures that only those states that were initially occupied on the left and empty on the right contribute to the current flowing from left to right,  $J_{L \rightarrow R}$ , which adopts the form

$$J_{L \rightarrow R} = \frac{e}{L} \sum_k v(k) T(k) f_L(k) [1 - f_R(k)]. \quad (3.7)$$

Now, we can convert the sum into an integral with the usual replacement:  $(1/L) \sum_k g(k) \rightarrow 1/(2\pi) \int g(k) dk$ . Thus,

$$J_{L \rightarrow R} = \frac{e}{2\pi} \int dk v(k) T(k) f_L(k) [1 - f_R(k)]. \quad (3.8)$$

We now change from the variable  $k$  to energy,  $E$ , introducing the density of states  $dk/dE = (dE/dk)^{-1} = m/(\hbar^2 k)$ , since  $E = \hbar^2 k^2 / (2m)$ .<sup>3</sup> Due to the cancellation between the group velocity and the density of states, the left-to-right current can be written as

$$J_{L \rightarrow R} = \frac{e}{h} \int dE T(E) f_L(E) [1 - f_R(E)]. \quad (3.9)$$

Analogously, we can show that the current from right to left can be written as

$$J_{R \rightarrow L} = \frac{e}{h} \int dE T(E) f_R(E) [1 - f_L(E)], \quad (3.10)$$

where we have used the fact that the transmission probability is the same, no matter in which direction the barrier is crossed.

Now, the total current<sup>4</sup>  $I(V) = J_{L \rightarrow R} - J_{R \rightarrow L}$  can be simply expressed as

$$I(V) = \frac{2e}{h} \int_{-\infty}^{\infty} dE T(E, V) [f_L(E) - f_R(E)] \quad (3.11)$$

Here, we have introduced an extra factor 2 to account for the spin degeneracy which usually exists in the systems that we shall analyze, and by writing  $T(E, V)$  we want to stress the fact that the transmission can also depend on the bias voltage. This expression is the simplest version of the so-called *Landauer formula* and it illustrates the close relation between current and transmission.

Let us remind that the Fermi functions appearing in Eq. (3.11) are given by

$$f_{\alpha}(E) = \frac{1}{1 + e^{(E - \mu_{\alpha})/k_B T}}, \quad (3.12)$$

where  $\alpha = L, R$  and  $\mu_{L,R} = \mu \mp eV/2$ ,  $\mu$  being the equilibrium chemical potential of the system. At zero temperature  $f_L(E)$  and  $f_R(E)$  are step functions, equal to 1 below  $E_F + eV/2$  and  $E_F - eV/2$ , respectively, and 0 above this energy. If we moreover assume low voltages (linear regime), this expression reduces to  $I = GV$ , where the conductance is

$$G = (2e^2/h)T(E_F, V = 0) \quad (3.13)$$

<sup>3</sup>Here, we are assuming that the conduction electrons can be described by a non-interacting electron (or Fermi) gas.

<sup>4</sup>Since we are in a 1D situation, there is no difference between total current and current density.

Here,  $T(E_F, V = 0)$  is the zero-bias transmission evaluated at the Fermi energy.

This simple calculation demonstrates that a perfect single mode conductor between two electrodes has a finite resistance, given by the universal quantity  $h/2e^2 \approx 12.9 \text{ k}\Omega$ . This is an important difference with respect to macroscopic leads, where one expects to have zero resistance for the perfectly conducting case. This result might be a bit shocking, but with a little bit of thinking one can conclude that the finite resistance is associated with the resistance arising at the interfaces between the leads and the sample.

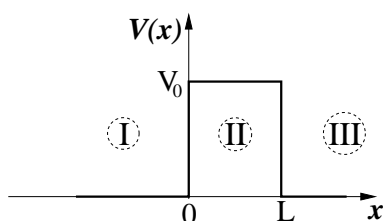
### 3.3 Penetration of a potential barrier: Tunnel effect

As it is clear from Eq. (3.11), the transmission probability plays a central role in Landauer approach. For this reason, it is worth reminding how this quantum mechanical quantity can be computed in some simple situations of special interest. For the sake of concreteness, we shall focus our discussion on this section in the analysis of the transmission through a single potential barrier. This simple problem not only illustrates some fundamental issues, but it also provides basic models which are widely used for the description of tunneling currents in a great variety of situations such as tunnel junctions based on insulating barriers, STM, and even single-molecule junctions.

Let us consider the rectangular potential barrier of height  $V_0$  depicted in Fig. 3.3. Our goal is to compute the probability for an incoming electron to cross such a barrier as a function of the energy,  $E$ . Classical mechanics tell us that an incident particle will always be reflected when  $E < V_0$ , and it will always be transmitted when  $E > V_0$ . We all know that in quantum mechanics a particle can pass through a barrier, even when its energy is lower than the barrier height. This phenomenon is known as *quantum tunneling* or simply *tunnel effect* and it lies at the heart of the whole physics discussed in this course.

In order to compute the transmission we proceed in the standard way. We first determine the wave functions in the three different regions defined in Fig. 3.3, and then we match these functions and their first spatial derivatives at the boundaries ( $x = 0$  and  $x = L$ ). Let us first consider the case of  $E < V_0$ . In this case, the solutions of the Schrödinger equation in the three regions are of the form

$$\psi_{\text{I}} = a_1 e^{ik_1 x} + b_1 e^{-ik_1 x}, \quad \psi_{\text{II}} = a_2 e^{k_2 x} + b_2 e^{-k_2 x}, \quad \psi_{\text{III}} = a_3 e^{ik_3 x}, \quad (3.14)$$

Fig. 3.3 Rectangular potential barrier of height  $V_0$  and width  $L$ .

where

$$k_1 = k_3 = \frac{\sqrt{2mE}}{\hbar} \quad \text{and} \quad k_2 = \frac{\sqrt{2m(V_0 - E)}}{\hbar}. \quad (3.15)$$

Note that we have assumed that the effective mass is the same everywhere and we have discarded the incoming term ( $b_3 e^{-ik_3 x}$ ) in  $\psi_{\text{III}}$  because we are considering here the problem of a wave function impinging on the barrier from the left.

Using now the continuity of the wave function and its first derivative at  $x = 0$  and  $x = L$ , we arrive at the following relationships

$$\begin{aligned} a_1 + b_1 &= a_2 + b_2 ; \quad ik_1 a_1 - ik_1 b_1 = k_2 a_2 - k_2 b_2 & (3.16) \\ a_2 e^{k_2 L} + b_2 e^{-k_2 L} &= a_3 e^{ik_1 L} ; \quad k_2 a_2 e^{k_2 L} - k_2 b_2 e^{-k_2 L} = ik_1 a_3 e^{ik_1 L}. \end{aligned}$$

Solving these equations, we obtain the following expression for the energy dependence of the transmission coefficient

$$T = \left| \frac{a_3}{a_1} \right|^2 = \frac{1}{1 + \left( \frac{k_1^2 + k_2^2}{2k_1 k_2} \right)^2 \sinh^2(k_2 L)} = \frac{4E(V_0 - E)}{4E(V_0 - E) + V_0^2 \sinh^2(k_2 L)}. \quad (3.17)$$

Proceeding in a similar way, one can compute the transmission for  $E > V_0$  and the result is (see Exercise 3.2)

$$T = \frac{1}{1 + \left( \frac{k_1^2 - k_2^2}{2k_1 k_2} \right)^2 \sin^2(k_2 L)} = \frac{4E(E - V_0)}{4E(E - V_0) + V_0^2 \sin^2(k_2 L)}. \quad (3.18)$$

The energy and length dependence of the transmission of this potential barrier are illustrated in Fig. 3.4. The most prominent feature is maybe the exponential dependence of the transmission on the barrier width for energies  $E < V_0$ , see Fig. 3.4(b). According to Eq. (3.17), this decay is given by  $T \propto \exp(-2k_2 L) = \exp(-2L\sqrt{2m(V_0 - E)}/\hbar)$ , i.e. the slopes in Fig. 3.4(b) are mainly determined by the square root of the difference

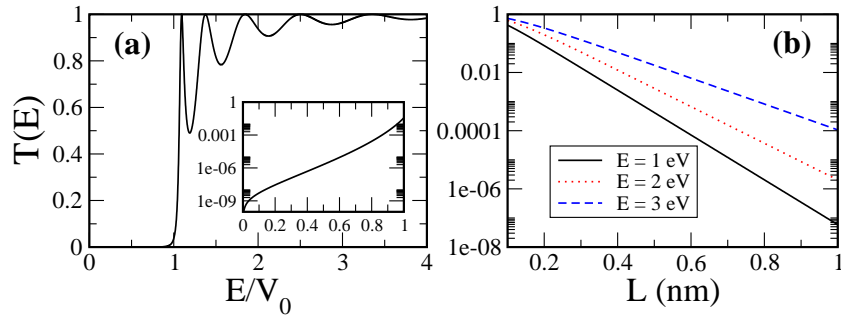


Fig. 3.4 (a) Transmission probability vs. energy for a symmetric potential barrier of height  $V_0 = 4$  eV and width  $L = 1$  nm. The inset shows a blow-up of the region  $E < V_0$ . (b) Transmission as a function of the width of the potential barrier ( $V_0 = 4$  eV) for different values of the energy. In both cases the mass is assumed to be the electron mass.

between the electron energy and the barrier height. Since the transmission determines the conductance, this model provides a natural explanation for the exponential decay of the low-bias conductance as a function of the distance between the electrodes in all kind of tunnel barriers. It also tells us that such decay is simply governed by the work function of the metals involved.

Landauer formula shows that the linear conductance at low temperatures is determined by the transmission at the Fermi energy. However, the analysis of the current-voltage (I-V) characteristics requires the knowledge of the energy dependence and, strictly speaking, also of the voltage dependence of the transmission probability, see Eq. (3.11). In the case of a rectangular barrier, the voltage can be introduced in an approximate way as shown in Fig. 3.5(a). The computation of the transmission and in turn of the I-V curves is then a simple problem, see Exercise 3.3. A more appropriate way of describing the effect of the voltage is shown in Fig. 3.5(b), where a linear drop in the potential with the barrier region has been assumed.

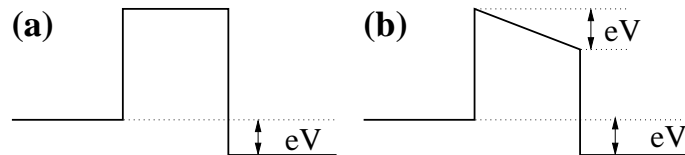


Fig. 3.5 Rectangular potential barrier under the application of a voltage: (a) approximation and (b) actual potential profile.

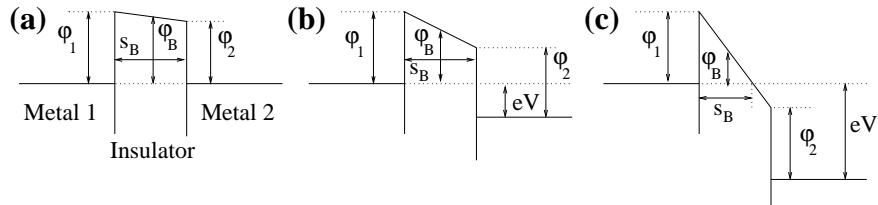


Fig. 3.6 Tunneling through a junction in which two metallic electrodes are separated by a thin insulating film, which is modeled as a rectangular potential barrier. The three panels show the three distinct voltage ranges discussed in the text.

The analysis of the transmission through a potential like the one of Fig. 3.5(b), or any other smooth barrier, can be tackled with the help of the WKB approximation [7] (see also Exercise 3.4). This is precisely what Simmons did in 1963 [8] in his celebrated model. He considered the problem of the tunnel effect between metallic electrodes separated by a thin insulating film. He derived a general formula for the I-V curves for a barrier of arbitrary shape, and we reproduce here his result for the particular case of a rectangular barrier. Simmons showed that zero-temperature net current density in this case can be written as [8]

$$J = J_0 \left\{ \varphi_B \exp(-A\sqrt{\varphi_B}) - (\varphi_B + eV) \exp(-A\sqrt{\varphi_B + eV}) \right\}, \quad (3.19)$$

where  $\varphi_B$  is the average barrier height relative to the negative electrode and  $s_B$  is the barrier width  $s_B$ , see Fig. 3.6. Moreover,

$$A = \frac{2\alpha s_B}{\hbar} \sqrt{2m} \quad \text{and} \quad J_0 = \frac{e}{2\pi\hbar\alpha^2 s_B^2}, \quad (3.20)$$

where  $\alpha$  is a dimensionless correction factor of order unity. Eq. (3.19) can be simplified in three distinct cases depending on the applied voltage:

**Low-voltage range.** For very small voltages ( $eV \sim 0$ ), see Fig. 3.6(a), the average barrier height  $\varphi_B$  is independent of the applied voltage and equals the zero voltage barrier height  $\varphi_0 = (\varphi_1 + \varphi_2)/2$ . Then, Eq. (3.19) can be simplified into

$$J = J_L V \quad \text{with} \quad J_L = \frac{e^2 \sqrt{2m\varphi_B}}{4\pi^2 \alpha \hbar^2 s_B} \exp(-A\sqrt{\varphi_B}). \quad (3.21)$$

Here,  $\alpha = 1$ . As it can be seen in Eq. (3.21), the current density is a linear function of the applied voltage  $V$  (Ohmic regime).

**Intermediate-voltage range.** For a medium applied voltage  $eV < \varphi_0$ , see Fig. 3.6(b), the average barrier height  $\varphi_B$  is given by  $(\varphi_1 + \varphi_2 - eV)/2$ .

The current density can then be simplified to (assuming that  $\alpha = 1$ )

$$J = J_L(V + \gamma V^3) \quad \text{with} \quad \gamma = \frac{(Ae)^2}{96\varphi_0} - \frac{Ae^2}{32\varphi_0^{3/2}}. \quad (3.22)$$

This expression can be used to determine both the height and the barrier width in terms of the coefficients  $\gamma$  and  $J_L$ .

**High-voltage range.** For voltages  $eV > \varphi_0$ , see Fig. 3.6(c), the average barrier height is reduced to  $\varphi_1/2$  and even the barrier width is reduced. Eventually, the voltage is high enough so that the Fermi level of electrode 2 is lower than the conduction band of electrode 1. In this case, tunneling from electrode 2 in electrode 1 is not possible since there are no empty states in electrode 1 to tunnel to. As for electrons tunneling from electrode 1 into electrode 2, all states in electrode 2 are empty. This is analog to field emission from a metal into vacuum. Then, the current density can be simplified to

$$J = \frac{2.2e^3}{8\pi h} \frac{F^2}{\varphi_1} \exp\left(-\frac{8\pi\sqrt{2m}\varphi_1^{3/2}}{2.96ehF}\right), \quad (3.23)$$

with the electric field strength in the insulator  $F = V/s$ , where  $s$  is the thickness of the insulating field.

In the case of vacuum tunneling (or tunneling through an insulator), we should be aware of the fact that whilst the electron is in the tunnel gap, it will induce image charges in the two electrodes. This serves to modify the barrier potential. The net effect of this is to reduce the average barrier height and hence increase the transmission probability. For an analysis of these “image forces” for the case of the rectangular barrier discussed here, see Ref. [8].

It is worth mentioning that the problem of the rectangular barrier under an applied voltage, see Fig. 3.5(b), can be solved exactly using the full Airy functions. This was done by Gundlach [9], who showed that the current exhibits oscillations as a function of voltage that are superimposed in the WKB result discussed above.

### 3.4 The scattering matrix

In section 3.6 we shall present a more rigorous discussion of the scattering formalism, where the concept of scattering matrix plays a central role. The definition and properties of this matrix are described in many quantum

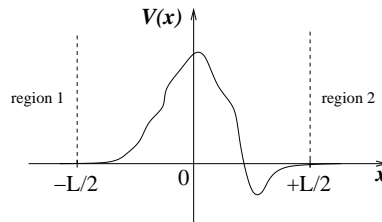


Fig. 3.7 The potential  $V(x)$  under consideration varies in an arbitrary way within the interval  $-L/2 \leq x \leq +L/2$  and goes to zero outside this interval.

mechanics textbooks, but for the sake of completeness, we have included here a brief discussion of this subject.

### 3.4.1 Definition and properties of the scattering matrix

In order to keep our discussion at a simple level, we study here a one-dimensional situation. Let us consider a potential  $V(x)$  which is zero outside the region defined by  $|x| > L/2$ , but which varies in an arbitrary way inside this interval, see Fig. 3.7. The equation satisfied by every wave function  $\psi(x)$  associated with a stationary state of energy  $E$  is

$$\left\{ \frac{d^2}{dx^2} + \frac{2m}{\hbar^2} [E - V(x)] \right\} \psi(x) = 0. \quad (3.24)$$

The most general solution  $\psi(x)$  of Eq. (3.24) in the region  $x < -L/2$  (region 1) for a given value of  $E$  can be written as

$$\psi_k(x) = a_1 e^{ikx} + b_1 e^{-ikx}, \quad (3.25)$$

where  $k = \sqrt{2mE/\hbar^2}$ , while in the region  $x > +L/2$  (region 2) it has the form

$$\psi_k(x) = a_2 e^{-ikx} + b_2 e^{ikx}, \quad (3.26)$$

Here, the different coefficients depend on  $k$ , as well as on the shape of the potential under study. Notice that with our notation, the amplitudes  $a_i$  ( $i = 1, 2$ ) correspond to the incoming waves impinging on the potential region, whereas the amplitudes  $b_i$  correspond to the outgoing waves.

The scattering matrix is defined as the  $2 \times 2$  matrix that relates the incoming and outgoing amplitudes as follows

$$\begin{pmatrix} b_1 \\ b_2 \end{pmatrix} = \hat{S} \begin{pmatrix} a_1 \\ a_2 \end{pmatrix}, \quad (3.27)$$

where  $\hat{S}$  is usually written as

$$\hat{S} = \begin{pmatrix} r & t' \\ t & r' \end{pmatrix}. \quad (3.28)$$

Here,  $r$  and  $r'$  are reflection amplitudes and  $t$  and  $t'$  are the transmission amplitudes associated to this potential.

Are all these four elements independent? What are the properties of the scattering matrix? A first property of the  $S$ -matrix can be deduced from the conservation of the current. Let us remind that in quantum mechanics, the current associated with a wave function  $\psi(x)$  is given by

$$J(x) = \frac{\hbar}{2mi} \left[ \psi^*(x) \frac{d\psi}{dx} - \psi(x) \frac{d\psi^*}{dx} \right]. \quad (3.29)$$

Differentiating, we find

$$\frac{d}{dx} J(x) = \frac{\hbar}{2mi} \left[ \psi^*(x) \frac{d^2\psi}{dx^2} - \psi(x) \frac{d^2\psi^*}{dx^2} \right]. \quad (3.30)$$

Taking into account Eq. (3.24), we obtain

$$\frac{d}{dx} J(x) = 0. \quad (3.31)$$

Therefore, the current  $J(x)$  associated with a stationary state is the same at all points of the  $x$ -axis. Note, moreover, that Eq. (3.31) is simply the one-dimensional analog of the relation (continuity equation)

$$\nabla \cdot \mathbf{J}(\mathbf{r}) = 0, \quad (3.32)$$

which is valid for any stationary state of a particle moving in three-dimensional space. According to Eq. (3.31), the current  $J(x)$  has the same value, no matter in which region it is evaluated. Then, computing the current in regions 1 and 2 we have

$$J(x) = \frac{\hbar k}{m} [|a_1|^2 - |b_1|^2] = \frac{\hbar k}{m} [|b_2|^2 - |a_2|^2], \quad (3.33)$$

which implies that

$$|a_1|^2 + |a_2|^2 = |b_1|^2 + |b_2|^2. \quad (3.34)$$

This relation can be used to establish the first property of the scattering matrix in the following way

$$\begin{aligned} |b_1|^2 + |b_2|^2 &= (b_1^*, b_2^*) \begin{pmatrix} b_1 \\ b_2 \end{pmatrix} = (a_1^*, a_2^*) \hat{S}^\dagger \hat{S} \begin{pmatrix} a_1 \\ a_2 \end{pmatrix} = \\ &= (a_1^*, a_2^*) \begin{pmatrix} a_1 \\ a_2 \end{pmatrix} = |a_1|^2 + |a_2|^2, \end{aligned} \quad (3.35)$$

which simply implies that  $\hat{S}$  is an unitary matrix, i.e.

$$\hat{S}^\dagger = \hat{S}^{-1}. \quad (3.36)$$

In terms of the matrix elements, this relation reads

$$\begin{aligned} |r|^2 + |t|^2 &= 1 ; r^*t' + t^*r' = 0 \\ (t')^*r + (r')^*t &= 0 ; |r'|^2 + |t'|^2 = 1. \end{aligned} \quad (3.37)$$

Notice that the second and third relations are indeed the same.

If the potential  $V(x)$  is real, which means in particular that there is no magnetic field applied, an additional property can be derived as follows. If  $\psi(x)$  is a solution of Eq. (3.24), then  $\psi^*(x)$  is also a solution. This new solution can be written as

$$\begin{aligned} \psi^*(x) &= a_1^* e^{-ikx} + b_1^* e^{ikx} & \text{if } x < -L/2 \\ \psi^*(x) &= a_2^* e^{ikx} + b_2^* e^{-ikx} & \text{if } x > +L/2. \end{aligned}$$

Notice that in this solution the coefficients  $a_i^*$  correspond to the outgoing amplitudes, while  $b_i^*$  represent the incoming amplitudes. Therefore, by definition they are related via the scattering matrix as follows

$$\begin{pmatrix} a_1^* \\ a_2^* \end{pmatrix} = \hat{S} \begin{pmatrix} b_1^* \\ b_2^* \end{pmatrix}, \quad (3.38)$$

which can be rewritten as

$$\begin{pmatrix} b_1 \\ b_2 \end{pmatrix} = (\hat{S}^*)^{-1} \begin{pmatrix} a_1 \\ a_2 \end{pmatrix}, \quad (3.39)$$

If we now compare this relation with Eq. (3.27), we arrive at

$$(\hat{S})^{-1} = \hat{S}^*. \quad (3.40)$$

If we now combine this with the fact that the scattering matrix is unitary, we have that  $\hat{S}$  is symmetric

$$(\hat{S})^T = \hat{S} \Rightarrow t' = t. \quad (3.41)$$

In the presence of a magnetic field, this latter relation changes and one can show that reversing the magnetic field  $B$  transposes the S-matrix

$$\hat{S}(B) = \hat{S}^T(-B) \Rightarrow t'(B) = t(-B). \quad (3.42)$$

The demonstration is left as an exercise (see Exercise 3.7).

### 3.4.2 Combining scattering matrices

It is interesting to discuss how one can combine different scattering matrices in a problem in which there are several scattering potentials. Let us for instance consider the case of two potential barriers of arbitrary shape. This situation is schematically represented in Fig. 3.8. We shall include in the scattering matrix a superindex indicating to which potential barrier it corresponds,  $\hat{S}^{(i)}$  ( $i = 1, 2$ ). These matrices  $\hat{S}^{(i)}$  relate the incoming and outgoing amplitudes across the corresponding potential barrier as follows (see Fig. 3.8)

$$\begin{pmatrix} b_1 \\ b_2 \end{pmatrix} = \hat{S}^{(1)} \begin{pmatrix} a_1 \\ a_2 \end{pmatrix}; \quad \begin{pmatrix} a_2 \\ b_3 \end{pmatrix} = \hat{S}^{(2)} \begin{pmatrix} b_2 \\ a_3 \end{pmatrix}. \quad (3.43)$$

Notice that we have already used the fact that  $a_2$  is at the same time the incoming amplitude for the potential 1 and the outgoing amplitude for potential 2. Something similar happens with  $b_2$ .

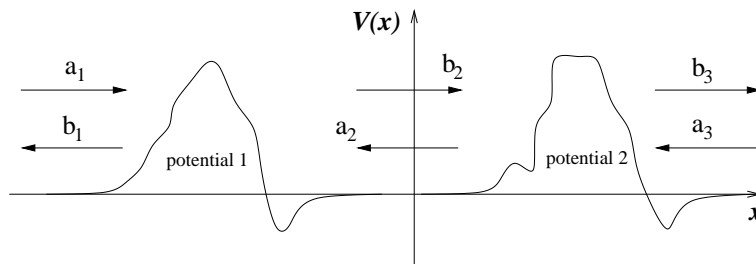


Fig. 3.8 Combination of two potential barriers of arbitrary shape. The coefficients  $a_i$  and  $b_i$  represent the different incoming and outgoing amplitudes with respect to the potential barrier  $i$ .

Our problem is to find in terms of the matrix elements of  $\hat{S}^{(i)}$  the total scattering matrix  $\hat{S}_{\text{Tot}}$  that relates the incoming and outgoing amplitudes of the two scatterers, i.e.

$$\begin{pmatrix} b_1 \\ b_3 \end{pmatrix} = \hat{S}_{\text{Tot}} \begin{pmatrix} a_1 \\ a_3 \end{pmatrix}; \quad \hat{S}_{\text{Tot}} = \begin{pmatrix} r & t' \\ t & r' \end{pmatrix}. \quad (3.44)$$

This can be easily done eliminating  $a_2$  and  $b_2$  from Eq. (3.43) and the final result can be written as

$$\begin{aligned} r &= r^{(1)} + t'^{(1)} r^{(2)} \left[ 1 - r'^{(1)} r^{(2)} \right]^{-1} t^{(1)}; \quad t = t^{(2)} \left[ 1 - r'^{(1)} r^{(2)} \right]^{-1} t^{(1)} \\ r' &= r'^{(2)} + t^{(2)} \left[ 1 - r'^{(1)} r^{(2)} \right]^{-1} r'^{(1)} t'^{(2)}; \quad t' = t'^{(1)} \left[ 1 - r^{(2)} r'^{(1)} \right]^{-1} t'^{(2)}. \end{aligned} \quad (3.45)$$

This result allows us to compute now very easily, for instance, the total transmission through the combined structure. According to the previous equations

$$T = |t|^2 = \frac{T_1 T_2}{1 - 2\sqrt{R_1 R_2} \cos \theta + R_1 R_2}, \quad (3.46)$$

where  $T_i = |t^{(i)}|^2 = |t'^{(i)}|^2$ ,  $R_i = |r^{(i)}|^2 = |r'^{(i)}|^2$  and  $\theta = \text{phase}(r'^{(1)}) + \text{phase}(r^{(2)})$  is the phase shift acquired in one round-trip between the scatterers. This formula will be used in the next section to study the resonant tunneling.

### 3.5 Resonant tunneling

The phenomenon known as *resonant tunneling*, i.e. the tunneling through a localized energy level, takes place in numerous nanodevices ranging from semiconductor quantum wells to quantum dots and it is specially important in the context of molecular electronics. For this reason, we shall make a first approach to this phenomenon here and we shall come back to this issue in later chapters.

Let us consider a system described by a potential containing two barriers separated by a distance  $d$ . For the sake of concreteness, we assume that the two potential barriers are identical and they have a rectangular shape with height equal to  $V_0$  and width equal to  $L$ . We are now interested in the transmission probability for an electron to cross this system. This probability can be easily computed with the help of Eq. (3.46) and the results of section 3.3 (see also Exercise 3.8). An example of the energy dependence of the transmission for this double-barrier system is shown in Fig. 3.9, where we have assumed that  $V_0 = 4$  eV,  $L = 2$  Å and  $d = 2$  nm. As you can see, the most prominent feature is the appearance of a series of sharp resonances where the transmission goes all the way up to 1. It is easy to show that in the limit in which the resonances are well separated, which occurs when the barriers are rather opaque, the energy dependence of the transmission close to one of those resonances can be written as (see Exercise 3.8)

$$T(E) = \frac{4\Gamma^2}{(E - \epsilon_0)^2 + 4\Gamma^2}, \quad (3.47)$$

where  $\epsilon_0$  is the position in energy of the resonance and  $\Gamma = T_B/2(d\theta/dE)|_{E=\epsilon_0}$ . Here,  $T_B$  is the transmission through an individual

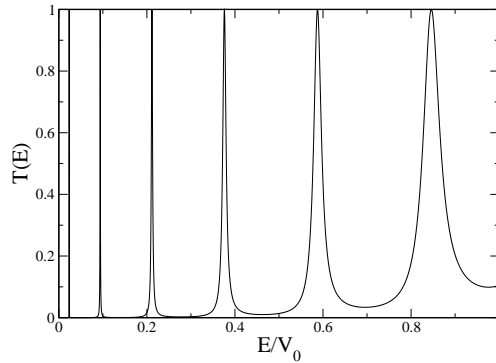


Fig. 3.9 Electron transmission as a function of energy for a system with two rectangular barriers of height  $V_0 = 4$  eV and width  $L = 2$  Å, which are separated by a distance  $d = 2$  nm.

rectangular barrier at energy  $E = \epsilon_0$ , which we have assumed to be much smaller than 1, and  $\theta(E) = 2kd$  is the round-trip phase shift appearing in Eq. (3.46), where  $k = \sqrt{2mE}/\hbar$  is the electron momentum in the region between the barriers. Eq. (3.47) tells us that the transmission close to the resonant conditions adopts a Lorentzian shape and its maximum is equal to 1, no matter how opaque the barriers are! This expression for the transmission is often referred to as the Breit-Wigner formula.

What is the physical origin of these resonances? It is easy to see that the occurrence of the maxima is described by the condition  $\cos \theta = 1$  [see Eq. (3.46)], which implies that  $k = n\pi/d$  with  $n = 0, 1, 2, \dots$ . This latter condition is nothing else but the condition satisfied by the eigenenergies of the problem of an infinite potential well of width  $d$ . This suggests that the transmission resonances are simply a manifestation of the fact that the electrons are tunneling through the energy levels (or bound states) of the central system (in this case a potential well). Strictly speaking, these states are no longer exact eigenstates of this system, but they acquire a finite lifetime given by  $\hbar/\Gamma$  in virtue of the coupling of the well to the external world via the potential barriers.

### 3.6 Multichannel Landauer formula

We present in this section a more rigorous derivation of Landauer formula, where the important concept of conduction channel will arise. This formulation is also the starting point for the extension of the scattering for-

malism to the description of other transport properties such as shot noise or thermoelectric coefficients (see Appendix B). This section is based on Refs. [10, 11].

We consider a mesoscopic sample connected to two reservoirs (terminals, probes), to be referred to as “left” (L) and “right” (R). It is assumed that the reservoirs are so large that they can be characterized by a temperature  $T_{L,R}$  and a chemical potential  $\mu_{L,R}$ ; the distribution functions of electrons in the reservoirs, defined via these parameters, are then Fermi distribution functions

$$f_\alpha(E) = [\exp[(E - \mu_\alpha)/k_B T_\alpha] + 1]^{-1}, \quad \alpha = L, R \quad (3.48)$$

(see Fig. 3.10). Far from the sample, we can assume that transverse (across the leads) and longitudinal (along the leads) motion of electrons are separable. In the longitudinal (from left to right) direction the system is open, and is characterized by the continuous wave vector  $k_l$ . It is advantageous to separate incoming (to the sample) and outgoing states, and to introduce the longitudinal energy  $E_l = \hbar^2 k_l^2 / 2m$  as a quantum number. Transverse motion is quantized and described by the discrete index  $n$  (corresponding to transverse energies  $E_{L,R,n}$ , which can be different for the left and right leads). These states are in the following referred to as *transverse (quantum) channels*. We write thus  $E = E_n + E_l$ . Since  $E_l$  needs to be positive, for a given total energy  $E$  only a finite number of channels exists. The number of incoming channels is denoted  $N_{L,R}(E)$  in the left and right lead, respectively.

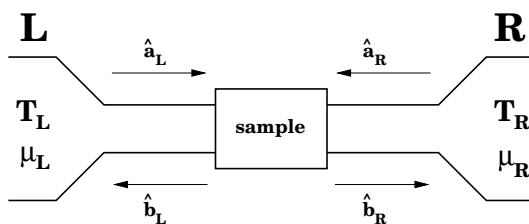


Fig. 3.10 Two-terminal scattering problem for the case of one transverse channel.

We now introduce *creation* and *annihilation operators* of electrons in the scattering states.<sup>5</sup> In principle, we could have used the operators which refer to particles in the states described by the quantum numbers  $n, k_l$ .

<sup>5</sup>The second quantization language will be used here at a very simple level. A discussion of this formalism is included in Appendix A and it will be widely used in the following chapters.

However, the scattering matrix relates current amplitudes and not wave function amplitudes. Thus, we introduce operators  $\hat{a}_{L_n}^\dagger(E)$  and  $\hat{a}_{L_n}(E)$  which create and annihilate electrons with total energy  $E$  in the transverse channel  $n$  in the left lead, which are incident upon the sample.<sup>6</sup> In the same way, the creation  $\hat{b}_{L_n}^\dagger(E)$  and annihilation  $\hat{b}_{L_n}(E)$  operators describe electrons in the outgoing states. They obey anti-commutation relations

$$\begin{aligned}\hat{a}_{L_n}^\dagger(E)\hat{a}_{L_{n'}}(E') + \hat{a}_{L_{n'}}(E')\hat{a}_{L_n}^\dagger(E) &= \delta_{nn'}\delta(E - E') \\ \hat{a}_{L_n}(E)\hat{a}_{L_{n'}}(E') + \hat{a}_{L_{n'}}(E')\hat{a}_{L_n}(E) &= 0 \\ \hat{a}_{L_n}^\dagger(E)\hat{a}_{L_{n'}}^\dagger(E') + \hat{a}_{L_{n'}}^\dagger(E')\hat{a}_{L_n}^\dagger(E) &= 0.\end{aligned}\quad (3.49)$$

Similarly, we introduce creation and annihilation operators  $\hat{a}_{R_n}^\dagger(E)$  and  $\hat{a}_{R_n}(E)$  for incoming states and  $\hat{b}_{R_n}^\dagger(E)$  and  $\hat{b}_{R_n}(E)$  for outgoing states in the right lead (Fig. 3.10).

The operators  $\hat{a}$  and  $\hat{b}$  are related via the scattering matrix  $\hat{S}$ ,

$$\begin{pmatrix} \hat{b}_{L1} \\ \vdots \\ \hat{b}_{LN_L} \\ \hat{b}_{R1} \\ \vdots \\ \hat{b}_{RN_R} \end{pmatrix} = \hat{S} \begin{pmatrix} \hat{a}_{L1} \\ \vdots \\ \hat{a}_{LN_L} \\ \hat{a}_{R1} \\ \vdots \\ \hat{a}_{RN_R} \end{pmatrix}.\quad (3.50)$$

The creation operators  $\hat{a}^\dagger$  and  $\hat{b}^\dagger$  obey a similar relation with the Hermitian conjugated matrix  $\hat{S}^\dagger$ .

The matrix  $\hat{S}$  has dimensions  $(N_L + N_R) \times (N_L + N_R)$ . Its size, as well as the matrix elements, depends on the total energy  $E$ . It has the block structure

$$\hat{S} = \begin{pmatrix} \hat{r} & \hat{t}' \\ \hat{t} & \hat{r}' \end{pmatrix}.\quad (3.51)$$

Here the square diagonal blocks  $\hat{r}$  (size  $N_L \times N_L$ ) and  $\hat{r}'$  (size  $N_R \times N_R$ ) describe electron reflection back to the left and right reservoirs, respectively. The off-diagonal, rectangular blocks  $\hat{t}$  (size  $N_R \times N_L$ ) and  $\hat{t}'$  (size  $N_L \times N_R$ ) are responsible for the electron transmission through the sample. The properties of the matrix  $\hat{S}$  are a straightforward generalization to a multi-mode case of those discussed in section 3.4. Thus for instance, the flux conservation in the scattering process implies that  $\hat{S}$  is quite generally

<sup>6</sup>We shall denote here the operators with a “hat” to distinguish them from the amplitudes of the previous section.

unitary. In the presence of time-reversal symmetry the scattering matrix is also symmetric.

The current operator in the left lead (far from the sample) is expressed in a standard way,

$$\hat{I}_L(z, t) = \frac{\hbar e}{2im} \int d\mathbf{r}_\perp \left[ \hat{\Psi}_L^\dagger(\mathbf{r}, t) \frac{\partial}{\partial z} \hat{\Psi}_L(\mathbf{r}, t) - \left( \frac{\partial}{\partial z} \hat{\Psi}_L^\dagger(\mathbf{r}, t) \right) \hat{\Psi}_L(\mathbf{r}, t) \right], \quad (3.52)$$

where the field operators  $\hat{\Psi}$  and  $\hat{\Psi}^\dagger$  are defined as

$$\hat{\Psi}_L(\mathbf{r}, t) = \int dE e^{-iEt/\hbar} \sum_{n=1}^{N_L(E)} \frac{\chi_{Ln}(\mathbf{r}_\perp)}{(2\pi\hbar v_{Ln}(E))^{1/2}} \left[ \hat{a}_{Ln} e^{ik_{Ln}z} + \hat{b}_{Ln} e^{-ik_{Ln}z} \right] \quad (3.53)$$

and

$$\hat{\Psi}_L^\dagger(\mathbf{r}, t) = \int dE e^{iEt/\hbar} \sum_{n=1}^{N_L(E)} \frac{\chi_{Ln}^*(\mathbf{r}_\perp)}{(2\pi\hbar v_{Ln}(E))^{1/2}} \left[ \hat{a}_{Ln}^\dagger e^{-ik_{Ln}z} + \hat{b}_{Ln}^\dagger e^{ik_{Ln}z} \right]. \quad (3.54)$$

Here  $\mathbf{r}_\perp$  is the transverse coordinate(s) and  $z$  is the coordinate along the leads (measured from left to right),  $\chi_n^L$  are the transverse wave functions, and we have introduced the wave vector,  $k_{Ln} = \hbar^{-1}[2m(E - E_{Ln})]^{1/2}$  (the summation only includes channels with real  $k_{Ln}$ ), and the velocity of carriers  $v_n(E) = \hbar k_{Ln}/m$  in the  $n$ -th transverse channel.

After some algebra, the expression for the current can be cast into the form<sup>7</sup>

$$\hat{I}_L(t) = \frac{e}{\hbar} \sum_n \int dE dE' e^{i(E-E')t/\hbar} \left[ \hat{a}_{Ln}^\dagger(E) \hat{a}_{Ln}(E') - \hat{b}_{Ln}^\dagger(E) \hat{b}_{Ln}(E') \right]. \quad (3.55)$$

Using Eq. (3.50) we can now express the current in terms of the  $\hat{a}$  and  $\hat{a}^\dagger$  operators alone,

$$\hat{I}_L(t) = \frac{e}{\hbar} \sum_{\alpha\beta} \sum_{mn} \int dE dE' e^{i(E-E')t/\hbar} \hat{a}_{\alpha m}^\dagger(E) A_{\alpha\beta}^{mn}(L; E, E') \hat{a}_{\beta n}(E'). \quad (3.56)$$

Here the indices  $\alpha$  and  $\beta$  label the reservoirs and may assume values  $L$  or  $R$ . The matrix  $A$  is defined as

$$A_{\alpha\beta}^{mn}(L; E, E') = \delta_{mn} \delta_{\alpha L} \delta_{\beta L} - \sum_k S_{L\alpha;mk}^\dagger(E) S_{L\beta;kn}(E'), \quad (3.57)$$

<sup>7</sup>Here, we have used the fact that the velocities  $v_n(E)$  vary with energy quite slowly, typically on the scale of the Fermi energy, and neglected their energy dependence.

and  $S_{L\alpha;mk}(E)$  is the element of the scattering matrix relating  $\hat{b}_{Lm}(E)$  to  $\hat{a}_{\alpha k}(E)$ . Note that Eq. (3.56) is independent of the coordinate  $z$  along the lead.

Let us now derive the average current from Eq. (3.56). For a system at thermal equilibrium the quantum statistical average of the product of an electron creation operator and annihilation operator of a Fermi gas is

$$\langle \hat{a}_{\alpha m}^\dagger(E) \hat{a}_{\beta n}(E') \rangle = \delta_{\alpha\beta} \delta_{mn} \delta(E - E') f_\alpha(E). \quad (3.58)$$

Using Eq. (3.56) and Eq. (3.58) and taking into account the unitarity of the scattering matrix  $\hat{S}$ , we obtain

$$I \equiv \langle \hat{I}_L \rangle = \frac{e}{h} \int_{-\infty}^{\infty} dE \operatorname{Tr} [\hat{t}^\dagger(E) \hat{t}(E)] [f_L(E) - f_R(E)]. \quad (3.59)$$

Here the matrix  $\hat{t}$  is the off-diagonal block of the scattering matrix,  $t_{mn} = S_{RL;mn}$ . In the zero-temperature limit and for a small applied voltage Eq. (3.59) gives a conductance

$$G = \frac{e^2}{h} \operatorname{Tr} [\hat{t}^\dagger(E_F) \hat{t}(E_F)], \quad (3.60)$$

where  $E_F$  is the Fermi energy. Eq. (3.60) establishes the relation between the scattering matrix evaluated at the Fermi energy and the conductance. It is a basis invariant expression. The matrix  $\hat{t}^\dagger \hat{t}$  can be diagonalized; it has a real set of eigenvalues (*transmission coefficients*)  $T_n(E)$  (not to be confused with temperature), each of them assumes a value between zero and one. The corresponding eigenfunctions will be referred to as *eigenchannels* or *conduction channels*. In this natural basis we have instead of Eq. (3.59)

$$I = \frac{e}{h} \sum_n \int_{-\infty}^{\infty} dE T_n(E) [f_L(E) - f_R(E)] \quad (3.61)$$

and thus for the zero-temperature linear conductance

$$G = \frac{e^2}{h} \sum_n T_n(E_F) \quad (3.62)$$

Eq. (3.62) is known as a multi-channel generalization of Landauer formula. Notice also that in the last formulas there is a difference of a factor 2 with respect to Eq. (3.11). The reason is that in the discussion above we have not assumed spin degeneracy.

For a constriction of only one atom in cross section one can estimate the number of conductance channels as  $N \simeq (k_F R/2)^2$ , which is between

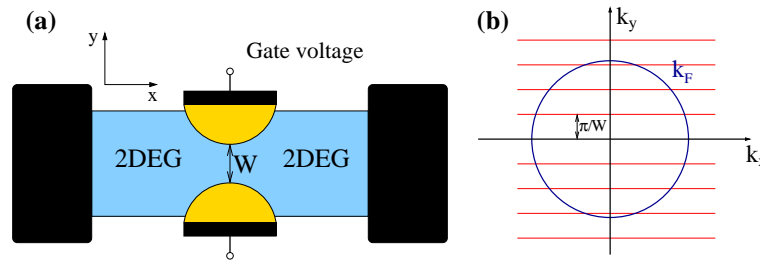


Fig. 3.11 (a) Schematic representation of a point contact defined in a two-dimensional electron gas (2DEG) by means of a split gate on top of the heterostructure. (b) Allowed states in the point contact constriction, which correspond to quantized values for  $k_y = \pm n\pi/W$ , and continuous values for  $k_x$ . The formation of these 1D subbands gives rise of a quantized conductance.

1 and 3 for most metals. We shall see that the actual number of channels is determined by the valence orbital structure of the atoms. In the case of molecular junctions, it turns out that, apart from a few notable exceptions, the conductance is dominated by a single conduction channel.

Let us emphasize that we have focused our discussion on a two-terminal configuration. The scattering approach was extended by Büttiker to describe the electronic transport in multi-terminal situations and this formalism (generally referred to as Landauer-Büttiker's formalism) has been widely used in the interpretation of mesoscopic experiments. We shall not discuss this generalization here and we refer you to Refs. [2, 10–12] for more details about this formalism.

### 3.6.1 Conductance quantization in 2DEG: Landauer formula at work

As a simple illustration of the use of Landauer formula, we shall now briefly discuss the conductance quantization in quantum point contacts defined in semiconductor hetero-structures (for a detailed discussion of this topic, see Refs. [13, 14]). It is well-known that in a semiconductor heterostructure like GaAs-AlGaAs one can confine the electrons in the two-dimensional interface between the two materials. Additionally, one can define electrostatically a point contact by means of a split gate on top of the heterostructure. This is schematically represented in Fig. 3.11(a). In this way one can define short and narrow constrictions in the two-dimensional electron gas (2DEG), of variable width  $0 < W < 250$  nm comparable to the Fermi wavelength  $\lambda_F \approx 40$  nm and much shorter than the mean free path  $l \approx 10$   $\mu$ m.

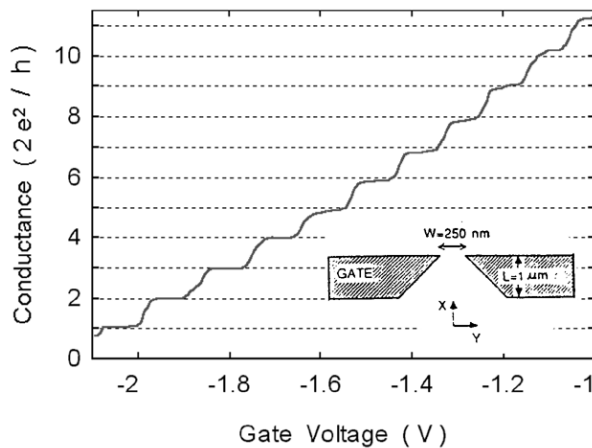


Fig. 3.12 Point contact conductance as a function of gate voltage at 0.6 K, demonstrating the conductance quantization in units of  $2e^2/h$ . The constriction width increases with increasing voltage on the gate (see inset). Reprinted with permission from [15]. Copyright 1988 by the American Physical Society.

Van Wees *et al.* [15] and Wharam *et al.* [16] independently discovered a sequence of steps in the conductance of such a point contact as its width was varied by means of the voltage on the split gate (see Fig. 3.12). The steps are near integer multiples of  $2e^2/h$ , after correction for a gate-voltage-independent series resistance from the wide 2DEG regions. This phenomenon is referred to as *conductance quantization*.

An elementary explanation of this effect relies on two facts: (i) the 2DEGs are ballistic systems (at least along the constriction) and the only scattering takes place against the potential walls defined by the split gates and (ii) the momentum of the electron is quantized in the transverse direction giving rise to 1D subbands. Since every subband that contributes to the transport (or conduction channel) has a perfect transparency and the number of them is obviously an integer, it follows from the two-terminal Landauer formula that the low temperature conductance  $G$  is quantized,

$$G = (2e^2/h)N, \quad (3.63)$$

as observed experimentally. Here,  $N$  is the total number of open conduction channels and the prefactor 2 accounts for the spin degeneracy. This number can be simply calculated assuming a square-well lateral confining potential of width  $W$ . In the constriction, the electron momentum along the transport direction ( $x$ -direction) can take any value, while the trans-

verse momentum  $k_y$  is quantized and can only take the following values:  $k_y = \pm n\pi/W$  with  $n = 1, 2, \dots, N$ , see Fig. 3.11(b). Since the current is only carried by those electrons at the Fermi energy (or with momentum equal to the Fermi momentum  $k_F$ ), the number of subbands is simply given by  $N = \text{Int}[k_F W/\pi]$ . Therefore, a new subband is made available for transport every time the width of the gate is increased by approximately half of the Fermi wavelength. This explains the stair-like behavior seen in Fig. 3.12.

A detailed explanation of the necessary conditions to observe the conductance quantization requires a more rigorous treatment of the confinement potential and the corresponding analysis of the mode coupling at the entrance and exit of the constriction. A more realistic model is discussed in Exercise 3.9.

### 3.7 Final remarks and limitations of the scattering approach

The scattering formalism has been extended to study a great variety of transport properties. Thus for instance, as we show in Appendix B, this formalism allows us describing important quantities for the field of molecular electronics such as the current fluctuations and the thermoelectrical coefficients. Overall, this approach has been very successful explaining many basic transport phenomena in numerous types of nanostructures. For time reasons we have to end here our discussion of this formalism, and for more details we recommend the reviews of Refs. [11, 13] and the didactic book of S. Datta [2].

In spite of its great success, the scattering approach is far from being a complete theory of quantum transport. In this sense, it is important to be aware of its limitations. Among them we want to emphasize two of special interest for the scope of this course:

(i) The scattering approach gives no hints on how to compute the transmission or, more generally, the scattering matrix. In particular, it does not tell us how to determine the actual transmission of an atomic contact or a molecular circuit. In this sense, one might think that this formalism has merely replaced a problem by another. This would be, of course, unfair. The scattering approach can be combined with simple models, as we showed in section 3.3, or with more sophisticated techniques like random matrix theory [17] to predict the transport properties of a great variety of systems such as diffusive wires, chaotic cavities, superconducting nanostructures,

resonant tunneling systems, tunnel junctions, etc.

(ii) The scattering picture is an one-electron theory which is valid only as long as inelastic scattering processes can be neglected. In this formalism one assumes that the electron propagation is a fully quantum coherent process over the entire sample. According to normal Fermi-liquid theory, such a description would be strictly valid at zero temperature and only for electrons at the Fermi energy. At finite bias the coherent propagation may be limited by inelastic scattering processes due to electron-phonon and electron-electron collisions. The theoretical description of transport in situations where inelastic interactions play an important role requires more sophisticated methods like the Green's function techniques that will be described in the next chapters.

### 3.8 Exercises

**3.1 Transmission through a potential step:** Show that the transmission probability as a function of energy,  $E$ , for the potential step shown in Fig. 3.13 is given by

$$T(E) = \begin{cases} 4k_1 k_2 / (k_1 + k_2)^2 & \text{if } E > V_0 \\ 0 & \text{if } E < V_0 \end{cases}$$

where  $k_1 = \sqrt{2mE/\hbar^2}$ ,  $k_2 = \sqrt{2m(E - V_0)/\hbar^2}$  and  $m$  is the electron mass.

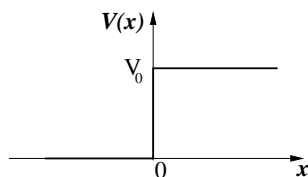


Fig. 3.13 Potential step of height  $V_0$ .

**3.2 Penetration of a rectangular barrier:** Show that the probability for an electron to cross the rectangular barrier shown in Fig. 3.3 for energies  $E > V_0$  is given by Eq. (3.18).

**3.3 A rectangular barrier under an applied voltage:** Consider the rectangular barrier under an applied bias shown in Fig. 3.5(a). Show that the energy and voltage dependence of the transmission for  $E < V_0$  is given by

$$T(E, V) = \frac{4k_1 k_2^2 k_3}{k_2^2 (k_1 + k_3)^2 + (k_1^2 + k_2^2)(k_2^2 + k_3^2) \sinh^2(k_2 L)},$$

where  $k_1 = \sqrt{2mE}/\hbar$ ,  $k_2 = \sqrt{2m(V_0 - E)}/\hbar$  and  $k_3 = \sqrt{2m(E + eV)}/\hbar$ .

Use this result and the Landauer formula [Eq. (3.11)] to compute the zero-temperature current-voltage characteristics for a barrier of height  $V_0 = 4$  eV and width  $L = 1$  nm.

### 3.4 Penetration of an arbitrary potential barrier:

(a) Let us consider a 1D potential barrier of arbitrary shape like the one depicted in Fig 3.14. The goal is to compute the transmission probability to tunnel through this barrier for a particle of mass  $m$  and total energy  $E$ . Show that when the energy is clearly below the maximum of  $V(x)$ , the transmission probability can be approximated by

$$T(E) \approx \exp\left(-2 \int_a^b \frac{\sqrt{2m[V(x) - E]}}{\hbar} dx\right),$$

where  $V(x)$  describes the potential and  $a$  and  $b$  are the classical turning points where  $V(x) = E$ . Hint: A barrier of arbitrary shape can be viewed as an infinite set of infinitesimally thin rectangular barriers in series. A more elegant way to address this problem is to use the WKB approximation, as shown, for instance, in Ref. [7].

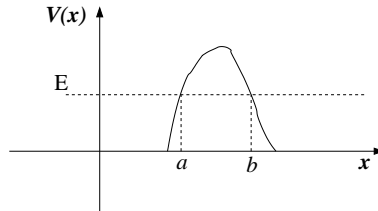


Fig. 3.14 Arbitrary potential barrier.

(b) In the spirit of Simmon's model, use the result obtained in (a) to study the zero-temperature current-voltage characteristics of a junction described by a trapezoidal barrier like the one shown in Fig 3.6. To be precise, obtain analytical results for the I–V curves in the limits of low and high voltage (see discussion of Simmon's model in section 3.3). Study numerically the shape of the I–V curves in the case in which  $\varphi_1 = \varphi_2 = 4$  eV,  $s_B = 1$  nm, and take for  $m$  the free electron mass.

**3.5 Resonant tunneling in a finite square well:** Analyze the transmission coefficient in the case of the square well shown in Fig 3.15. In particular, show that in the energy range  $E > V_3$  this coefficient is given by

$$T(E) = \frac{4k_1 k_3 k_2^2}{k_2^2 (k_1 + k_3)^2 \cos^2(k_2 L) + (k_2^2 + k_1 k_3)^2 \sin^2(k_2 L)},$$

where  $L = a - b$  and  $k_i$  is the electron momentum in the region  $i = \text{I, II, III}$ .

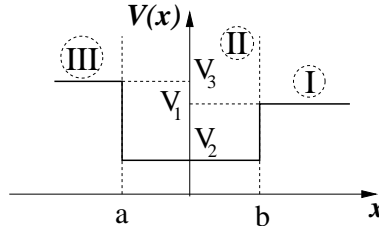


Fig. 3.15 Square well.

Show also that the transmission coefficient above exhibits resonances as a function of energy. In particular, calculate the position of those resonances and show that the transmission maxima are given by  $4k_1k_3/(k_1 + k_3)^2$ .

**3.6 Transmission through a delta function barrier:** Let us model a one-dimensional conductor with the following Hamiltonian

$$\mathbf{H} = -\frac{\hbar^2}{2m} \frac{\partial^2}{\partial x^2} + V_0 \delta(x),$$

where  $V_0$  is the strength of the delta potential that acts at  $x = 0$ .

(a) Demonstrate that the boundary conditions for the scattering states  $\psi_k(x)$ ,  $k$  being the electron momentum, are: (i) continuity at  $x = 0$  and (ii)  $\psi'_k(x = 0^+) - \psi'_k(x = 0^-) = (2mV_0/\hbar^2)\psi(x = 0)$ , where the prime symbol indicates derivative with respect to  $x$ .

(b) Use the previous result to show that the transmission probability through this delta potential can be expressed as:  $T = 1/(1 + Z^2)$ , where  $Z \equiv mV_0/(\hbar^2 k)$ .

**3.7 Scattering matrix:**

(a) Show that in the presence of a magnetic field the scattering matrix fulfills the property of Eq. (3.42).

(b) Derive the relations of Eq. (3.45).

**3.8 Resonant tunneling in a double-barrier system:** Consider a symmetric double barrier system formed by combining two rectangular barriers (see Exercise 3.2) of height  $V_0$  and width  $L$  that are separated a distance  $d$ .

(a) Compute the total transmission through this system for energies smaller than  $V_0$ . As a numerical example, reproduce the results of Fig. 3.9 where the following values were used:  $V_0 = 4$  eV,  $L = 2$  Å, and  $d = 2$  nm. Hint: Use the idea of the combination of scattering matrices, see Eq. (3.46) in section 3.4.2, and the result of Eq. (3.17).

(b) As in the case of the potential well of Exercise 3.5, the transmission in this double barrier system exhibits pronounced resonances. Find the position of those resonances and show that, in the limit in which they are well separated,

the transmission around one of those resonances can be written as

$$T(E) = \frac{4\Gamma^2}{(E - \epsilon_0)^2 + 4\Gamma^2},$$

where  $\epsilon_0$  is the position of the resonance and  $\Gamma$  is a scattering rate associated to the potential barriers. Find an expression for this rate in terms of the transmission of the barriers,  $T_B$ . Hints: (i) The resonances are well separated when the transmission  $T_B$  of the individual barriers is small. (ii) The round-trip phase shift that appears in Eq. (3.46) is  $\theta = 2kd$ , where  $k$  is the electron momentum in the region between the two barriers.

(c) Generalize the result obtained in (b) to the case of asymmetric barriers of arbitrary shape.

(d) Consider the example of Fig. 3.9 and use the Landauer formula to investigate the shape of the current-voltage characteristics in this case.

**3.9 Conductance quantization in a 2DEG:** One of the most successful applications of the Landauer formula is the explanation of the conductance quantization that takes place in split-gate constrictions (or quantum-point contacts) in a two-dimensional electron gas (2DEG). A useful model to study the occurrence of conductance steps is the so-called saddle point model used by Büttiker in Ref. [18]. In this model it is assumed that near the bottleneck of the constriction the electrostatic potential can be expressed as

$$V(x, y) = V_0 - \frac{1}{2}m\omega_x^2x^2 + \frac{1}{2}m\omega_y^2y^2. \quad (3.64)$$

Here,  $V_0$  is the electrostatic potential at the saddle,  $\omega_x$  characterizes the curvature of the potential barrier in the constriction and  $\omega_y$  the lateral confinement. Show that for this potential the transmission probabilities are given by

$$T_n(E) = \frac{1}{\exp[\pi(E - V_0 - (n + 1/2)\omega_x/\omega_y)] + 1}.$$

Using this expression in combination with the Landauer formula, find the criteria for the observation of well-defined conductance steps at low temperatures.



## Bibliography

- [1] R. Landauer, *Spatial variation of currents and fields due to localized scatterers in metallic conduction*, IBM J. Res. Dev. **1**, 223 (1957).
- [2] S. Datta, *Electronic Transport in Mesoscopic Systems*, (Cambridge University Press, Cambridge, UK, 1995).
- [3] J.C. Maxwell, *A treatise on electricity and magnetism*, volume 1, (Dover Publication, New York, USA, 1954).
- [4] Yu.V. Sharvin, *A possible method for studying Fermi surfaces*, Sov. Phys.-JETP **21**, 655 (1965) [Zh. Eksp. Teor. Fiz. **48**, 984 (1965)].
- [5] V.I. Fal'ko and G.B. Lesovik, *Quantum conductance fluctuations in 3d ballistic adiabatic wires*, Solid State Comm. **84**, 835 (1992).
- [6] J.A. Torres, J.I. Pascual, J.J. Saenz, *Theory of conduction through narrow constrictions in a three-dimensional electron gas*, Phys. Rev. B **49**, 16581 (1994).
- [7] A. Messiah, *Quantum Mechanics*, (Dover Publication, New York, USA, 1999).
- [8] J.G. Simmons, *Generalized formula for the electric tunnel effect between similar electrodes separated by a thin insulating film*, J. Appl. Phys. **34**, 1793 (1963).
- [9] K.H. Gundlach, *Zur Berechnung des Tunnelstroms durch eine trapezförmige Potentialstufe*, Solid-State Electron. **9**, 946 (1966).
- [10] M. Büttiker, *Scattering theory of current and intensity noise correlations in conductors and wave guides*, Phys. Rev. B **46**, 12485 (1992).
- [11] Ya. M. Blanter and M. Büttiker, *Shot noise in mesoscopic conductors*, Phys. Rep. **336**, 2 (2000).
- [12] M. Büttiker, *Role of quantum coherence in series resistors*, Phys. Rev. B **33**, 3020 (1986).
- [13] C.W.J. Beenakker, H. van Houten, *Quantum Transport in Semiconductor Nanostructures*, Solid State Physics **44**, 1 (1991).
- [14] H. van Houten, C.W.J. Beenakker, *Quantum Point Contacts*, Physics Today, p. 22, July (1996).
- [15] B.J. van Wees, H. van Houten, C.W.J. Beenakker, J.G. Williamson, L.P. Kouwenhoven, D. van der Marel, C.T. Foxon, *Quantized conductance of point contacts in a two-dimensional electron gas*, Phys. Rev. Lett. **60**, 848 (1988).

- [16] D.A. Wharam, T.J. Thornton, R. Newbury, M. Pepper, H. Ahmed, J.E.F. Frost, D.G. Hasko, D.C. Peacock, D.A. Ritchie, G.A.C. Jones, *One-dimensional transport and the quantisation of the ballistic resistance*, J. Phys. C **21**, L209 (1988).
- [17] C.W.J. Beenakker, *Random-matrix theory of quantum transport*, Rev. Mod. Phys. **69**, 731 (1997).
- [18] M. Büttiker, *Quantized transmission of a saddle-point constriction*, Phys. Rev. B **41**, 7906 (1990).